Bioorganic & Medicinal Chemistry Letters 21 (2011) 3658–3663

Contents lists available at ScienceDirect

Bioorganic & Medicinal Chemistry Letters

journal homepage: www.elsevier.com/locate/bmcl

From benzimidazole to indole-5-carboxamide Thumb Pocket I inhibitors of HCV NS5B polymerase. Part 1: Indole C-2 SAR and discovery of diamide derivatives with nanomolar potency in cell-based subgenomic replicons

Pierre L. Beaulieu [a,*], James Gillard [a], Eric Jolicoeur [a], Jianmin Duan [b], Michel Garneau [b], George Kukolj [b], Marc-André Poupart [a,†]

[a] Department of Chemistry, Boehringer Ingelheim (Canada) Ltd, Research and Development, 2100 Cunard Street, Laval (Québec), Canada H7S 2G5
[b] Department of Biological Sciences, Boehringer Ingelheim (Canada) Ltd, Research and Development, 2100 Cunard Street, Laval (Québec), Canada H7S 2G5

ARTICLE INFO

Article history:
Received 24 March 2011
Accepted 13 April 2011
Available online 20 April 2011

Keywords:
Hepatitis C virus
Antiviral
HCV
NS5B
Polymerase
Inhibitor
SAR

ABSTRACT

Replacement of the benzimidazole core of allosteric Thumb Pocket 1 HCV NS5B finger loop inhibitors by more lipophilic indole derivatives provided up to 30-fold potency improvements in cell-based subgenomic replicon assays. Optimization of C-2 substitution on the indole core led to the identification of analogs with EC_{50} <100 nM and modulated the pharmacokinetic properties of the inhibitors based on preliminary data from in vitro ADME profiles and in vivo rat PK.

The hepatitis C virus (HCV) is an RNA virus which is transmitted mostly through contaminated blood (e.g., intravenous drug users) and is thought to infect some 170 million individuals throughout the word. While the infection may remain asymptomatic for 20–30 years, approximately 20% of chronic carriers are at risk for eventually developing serious liver injuries such as cirrhosis and hepatocellular carcinomas (HCC).[1] Much progress has been realized toward the development of small molecule therapeutics (DAA: Direct Acting Antivirals), such as the NS3/4A protease inhibitors for the treatment of HCV infection.[2] However, the initial use of DAAs will be as an add-on to the current standard of care (SOC) combination of oral ribavirin (RBV) and subcutaneously administered pegylated interferon (PEG-IFN). Although the new treatment regimens have improved efficacies in treatment naïve patients infected with genotype 1 HCV, the PEG-IFN/RBV component is associated with severe side effects and these new therapies are only marginally efficacious against treatment-experienced null responders.[3]

Additional classes of DAAs are required to expand therapeutic options with alternative combinations that include all-oral PEG-IFN sparing regimens. Toward this end, we have been reporting on the discovery and optimization of specific allosteric inhibitors of the virally encoded NS5B RNA-dependent RNA polymerase (RdRp) of HCV. These benzimidazole derivatives bind in the thumb sub-domain of the polymerase and exert inhibition by interfering with the interaction of a loop that extends from the finger domain of the enzyme to a well defined pocket in the thumb. These '*finger-loop inhibitors*' thus interfere with conformational changes which are necessary for the formation of a RNA synthesis-competent state of the enzyme.[4] They represent a suitable class of compound that may be combined with the first wave of NS3/4A protease targeting DAAs to improve safety and efficacy in the treatment of chronic HCV infection.

We recently disclosed benzimidazole 5-carboxamide derivatives (e.g., **1**, Fig. 1) that feature an amino acid linker (e.g., D-Ala) between the left-hand-side benzimidazole core and a 4-aminocinnamic acid on the right-hand-side.[5] Further SAR, complemented with NMR and modeling studies established a conformational role for the central amino acid, providing rigidification of the backbone toward a presumed bioactive conformation. Incorporation of an α,α-disubstituted amino acid at this position enhanced inhibition of polymerase activity (e.g., **2**, IC_{50} = 40 nM).[6] However, despite significant advancements in intrinsic potency, the lack of improvement in cell-based subgenomic replicon activity[7] in this series

* Corresponding author.
E-mail address: pierre.beaulieu@boehringer-ingelheim.com (P.L. Beaulieu).
† Present address: Tranzyme Pharma, 3001 12ième Avenue Nord, Sherbrooke (Québec), Canada J1H 5N4.

0960-894X/$ - see front matter © 2011 Elsevier Ltd. All rights reserved.
doi:10.1016/j.bmcl.2011.04.059

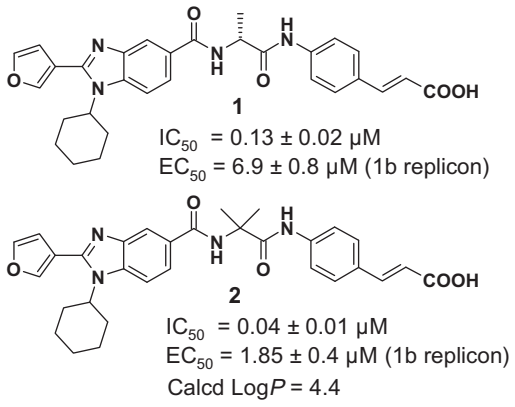

Figure 1. Thumb Pocket I benzimidazole inhibitors of HCV NS5B polymerase.

(EC_{50} >1 μM) jeopardized further progression of the benzimidazole derivatives toward development as potential drug candidates.

Recently, we and others reported the replacement of the benzimidazole core of truncated carboxylic acid versions of these inhibitors with more lipophilic indole isosteres. This modification provided enhanced cellular permeation and resulted in significant potency improvements in cell culture experiments.[8] When applied to benzimidazole 5-carboxamides such as **2**, this strategy increased cell culture activity 20–30-fold (compounds **3**–**5**, Table 1) despite small (two- to six-fold) apparent losses in intrinsic potency.

As shown in previous studies on truncated indole 5-carboxylic acid analogs,[8a] N-methylation of the indole (compound **4**) further improved potency. Alkylation with larger groups such as Et, *i*Bu or *i*Pr (not shown) did not provide additional benefit. While replacement of the benzimidazole scaffold by a *N*-methylindole provided a much needed boost in cellular activity (30-fold for **4** vs **2**), this change significantly increased lipophilicity. In the case of **4**, the calculated lipophilicity (Calcd Log *P* = 6.0) was 1.5 $\log_{10}$ greater than benzimidazole **2** (Calcd Log *P* = 4.4).[9] This deviation in drug-like attributes[10] was, in part, suspected to contribute to the low aqueous solubility of the compound at pH 7.2 (4 μg/mL),[11] modest metabolic stability in the presence of human liver microsomes (HLM $T_{1/2}$ = 29 min) and partial inhibition of CYP450 isozymes (2C9 IC_{50} = 2.4 μM; 2C19 IC_{50} = 4.2 μM; 2D6 IC_{50} = 9.0 μM; 3A4 IC_{50} = 8.7 μM).

Part 1 of this report describes optimization of the C-2 indole substituent that aimed to replace the furyl structural alert[12] in compound **4** with aryl and heterocyclic groups with the potential to reduce lipophilicity and improve physicochemical and ADME properties, while maintaining good cell culture activity. The accompanying Part 2 focuses on the central amino acid linker and right-hand-side SAR.[13]

Table 1
Indole diamides—N^1 SAR

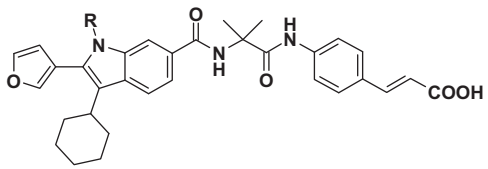

Compds	R	IC_{50}[a] (nM)	EC_{50}[a] (nM)	Calcd Log *P*[9]
3	H	172 ± 31	55, 121	5.7
4	Me	106 ± 22	54, 64	6.0
5	Et	282 ± 80	100	6.3
6	*i*Bu	623, 685	620	7.2

[a] n ⩾ 2: arithmetic mean ± standard deviation is reported.

The synthesis of inhibitors is depicted in Scheme 1. *N*-Alkylindole-5-carboxylic acid intermediates bearing various substituents at C-2 were prepared from 2-bromo- or 2-tributylstannyl indoles using palladium-catalyzed cross-coupling protocols as previously described.[8a] 2-Aminoisobutyric acid was coupled to ethyl 4-aminocinnamate via its acid chloride hydrochloride in the presence of pyridine as a base.[14] Coupling of this hindered amine to the indole carboxylic acid derivatives was performed under standard conditions using HATU and diisopropylethylamine in DMSO. Saponification using aqueous NaOH generated inhibitors that were purified by reversed-phase HPLC.[15]

Results for inhibitors bearing five-membered heterocycles, aromatic rings or heterobicyclic systems at the C-2 position of the indole scaffold are presented in Table 2 along with available data for metabolic stability in the presence of human liver microsomes (HLM), Caco-2 cell apical to basolateral permeability, solubility at pH 7.2 (amorphous solids) and Calcd Log *P*. As observed previously for benzimidazole-based inhibitors[16,8a] small five-membered heterocycles provided strongest inhibition of polymerase activity (compounds **4**, **8** and **9**). These compounds also displayed good potency in the cell-based replicon (EC_{50} = 45–60 nM). While solubility at pH 7.2 and Caco-2 permeability were acceptable for some of these analogs, metabolic stability remained an issue, particularly for thiazole **8** and oxazole **9**. Notably, substituted thiazole **10** also had good replicon potency despite significantly reduced activity against the enzyme assay (IC_{50} = 270 nM) and reasonable lipophilicity (Calcd Log *P* = 5.3). A similar profile was seen with a phenyl (**11**) or 4-chlorophenyl (**14**) substituent, displaying modest activity against the enzyme but good replicon potency. In general, substitution *ortho*- or *meta*- to the attachment point on the indole core negatively impacted intrinsic potency (IC_{50} >270 nM). We believe this is attributable to steric interactions that affect the conformation of the critical cyclohexyl moiety.[17] Nevertheless, the high lipophilicity of some analogs (e.g., **19**, **21**, and **23**) still resulted in relatively good activity in the benchmark replicon assay (EC_{50} <100 nM).

Achieving improvements in cell culture potency through increased lipophilicity was not a desirable strategy as such an approach would predictably compromise aqueous solubility and ADME-PK profile. This path could eventually lead to significant challenges for the development of such compounds. When six-membered heterocycles were introduced at C-2 of the indole core, more promising results were obtained as depicted in Table 3. 2-Pyridyl analog **24** had excellent intrinsic potency (IC_{50} = 36 nM), good cell-based activity (EC_{50} = 60 nM), excellent Caco-2 permeability and both solubility and lipophilicity were satisfactory. Unfortunately, metabolic stability in liver microsomes remained modest for this compound (HLM $T_{1/2}$ = 37 min). Further SAR was developed around this initial finding by scanning isomeric and substituted pyridines, as well as pyrimidines and pyrazines. The impact of modulating the pK_a[18] and lipophilicity of the C-2 substituent on potency and in vitro ADME parameters (metabolic stability and Caco-2 permeability) is shown in Table 3. The 2- and 4-pyridyl analogs **24** and **26** were two- to three-fold more potent in the replicon than the 3-pyridyl analog **25**, however the increased basicity of **26** had a negative impact on caco-2 permeability. Addition of methyl groups at various positions on the pyridine ring revealed that some substitution patterns were more tolerated than others. For example, and consistent with previous findings, substitution *ortho*- to the attachment point to the indole scaffold (compd **30**) was not tolerated. Interestingly, the sterically shielded *meta*-substituted pyridine **27** retained good potency and

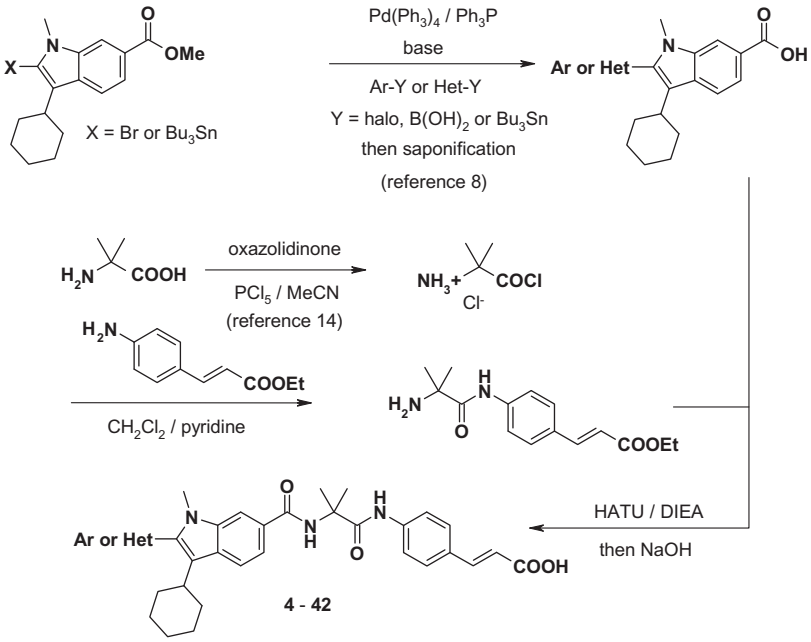

Scheme 1. Synthesis of indole-5-carboxamide inhibitors.

Caco-2 permeability, however the isomeric **28** was significantly less active in the polymerase assay. This finding suggests a preferred orientation for the pyridiyl nitrogen in the bound conformation that can only accommodate *meta*-substitution as displayed in isomer **27**. Unfortunately, analog **27** showed increased susceptibility to CYP450-mediated metabolism (HLM $T_{1/2}$ = 21 min). *para*-Substitution was well tolerated and compound **29** had a similar profile to unsubstituted pyridyl **24**. The substituted 3-pyridyl isomer **31** also had comparable potency to **24** or **29** however in this case, Caco-2 permeability was reduced. In an attempt to further decrease the lipophilicity of this class of inhibitors, polar amino functions were displayed on the pyridine contour (compounds **32**–**36**). Even with a substantial reduction in lipophilicity (Calcd Log *P* = 3.3 vs 4.9 for **24**) the 2-aminopyridyl analog **32** showed cell-based potency in the desired range (EC_{50} = 60 nM). Furthermore, the increased polarity of this analog improved metabolic stability in liver microsomes (HLM $T_{1/2}$ = 91 min). Unfortunately, the decrease in Calcd Log *P* also impacted Caco-2 permeability which was 10-fold lower relative to **24**. The addition of methoxy groups on the pyridyl ring reduced the pK_a of the nitrogen atom (compounds **37** and **38**), was relatively well tolerated for potency, and did not jeopardize metabolic stability or permeability. However, lipophilicity was increased substantially as suggested by Calcd Log *P* values >5.5. A trifluoromethyl group was somewhat tolerated potency wise (compd **39**), but further reduced basicity as lipophilicity increased to Calcd Log *P* = 6.1. As a result, metabolic stability and solubility were both compromised. Finally, introduction of an additional nitrogen atom into the C-2 indole substituent provided less basic pyrimidine and pyrazine analogs (**40**–**42**) with adequate lipophilicity (Calcd Log *P* = 4.2–4.7). Pyrazine **41** had good potency (comparable to pyridine **24**), caco-2 permeability and solubility. However, metabolic stability was reduced compared to the pyridyl analog.

Several representative analogs were also tested in a panel of CYP450 isozyme inhibition assays (1A2, 2C9, 2C19, 2D6 and 3A4). As a result of greater lipophilicity, indole-based inhibitors generally displayed increased inhibition of CYP450 enzymes compared to the corresponding benzimidazoles. For example, compound **1** did not inhibit 1A2, 2C9, 2C19 and 2D6 (IC_{50} >30 μM) and displayed only moderate inhibition of CYP3A4 (IC_{50} = 12.3 μM).[5a] In comparison, indole derivative **24** had IC_{50} = >30, 7.9, 2.7, 16.6, and 8.9 μM against the same panel of enzymes.

To summarize results presented in Tables 1–3, replacement of the benzimidazole scaffold in lead diamide derivative **2** by a more lipophilic *N*-methyindole isostere provided significant improvements in cell-based replicon potency and several analogs meeting our criteria for further advancement (EC_{50} <100 nM) were identified. Optimization of the C-2 indole substituent led to promising analogs such as compound **24** where the initial 3-furyl moiety was replaced by a less controversial pyridyl group while maintaining replicon potency and improving solubility. Overall lipophilicity was reduced in some cases to more acceptable values (Calcd Log *P* <5) while generally preserving Caco-2 permeability. However, metabolic stability in this class remained modest and moderate inhibition of CYP450 enzymes was observed (CYP3A4 IC_{50} = 5–15 μM).

Several representative inhibitors were also tested for specificity against another RNA-dependent RNA polymerase from polio virus and a mammalian DNA-dependent RNA polymerase II isolated from calf thymus.[7a] Selectivity indices (S.I.) were >150-fold in all cases.

In order to assess the potential of this class for oral exposure, two representative analogs (compound **24** and **32**) were selected for oral administration in rat (10 mg/kg dose).[19] Oral pharmacokinetic parameters are summarized in Table 4.

For both compounds, T_{max} was ⩽0.5 h, indicative of rapid absorption. For pyridyl analog **24**, maximum exposure (C_{max}) was reasonable as predicted from the good Caco-2 permeability. However, AUC was low and the oral MRT was short, indicative of rapid elimination, an observation that is consistent with the short measured $T_{1/2}$ = 9 min in the presence or rat liver microsomes. Compound **32** on the other hand had slightly improved metabolic stability that resulted in a longer MRT, but the reduced Caco-2 permeability only had a limited impact on oral exposure. These results indicate this class of compound is likely cleared through hepatic metabolism and that Caco-2 permeability is a good predictor of oral exposure. Part 2 of this account focuses on optimization of the central amino acid linker and the right-hand-side of the molecules and takes into account learnings from this initial investigation.[13]

Table 2
Indole 5-carboxamide C-2 SAR: five-membered heterocycles, heterobicycles and aryl groups

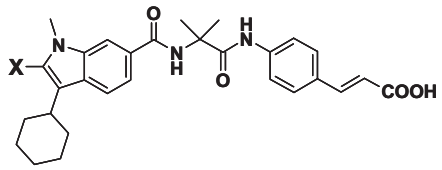

Compds	X	IC_{50}[a] (nM)	EC_{50}[a] (nM)	HLM $T_{1/2}$[b] (min)	Caco-2 (10^{-6}cm/s)	Solubility[11] pH 7.2 (μg/mL)	Calcd Log P[9]
4		106 ± 22	54, 64	29	6.0	4	6.0
7		180	56	100		< 0.1	6.2
8		46, 49	36, 64	29	8.5	39	5.2
9		34, 49	46	12	5.0	60	4.4
10	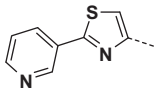	270	57	26	0.2	5	5.3
11		345	77				6.8
12		414	193				7.3
13	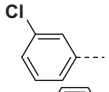	362	122				7.3
14	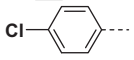	228	87	91		0.6	7.3
15	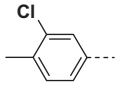	298	332				7.8
16	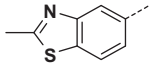	690					6.6
17	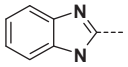	980	2800				4.9
18	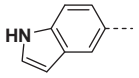	420	133				6.9
19	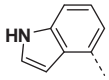	500	110				6.9
20		440					6.9
21	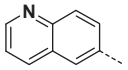	400	86	125	BDL	0.3	5.8
22	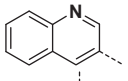	290	160				6.0
23	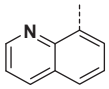	270	70	180	3.4	18	6.0

[a] $n \geqslant 2$: arithmetic mean ± standard deviation is reported.
[b] $T_{1/2}$ measured in human liver microsomes at 10 μM initial concentration.

Table 3
Indole 5-carboxamide C-2 SAR: six-membered heterocycles

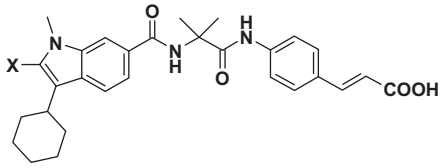

Compds	X	Calcd pK_a[18]	IC_{50}[a] (nM)	EC_{50}[a] (nM)	HLM $T_{1/2}$[b] (min)	Caco-2 (10^{-6}cm/s)	Solubility[11] pH 7.2 (μg/mL)	Calcd Log P[9]
24		5.4	36 ± 8	57, 62	37	16	50	4.9
25		5.3	109	144	25	9.4	34	4.4
26		6.0	110	46, 47	19	0.3	25	4.3
27		6.1	61, 91	36, 36	21	6.9	43	4.5
28		6.1	458, 543					4.9
29	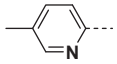	5.7	71	47		16.4	16	5.1
30		5.7	1000					5.0
31	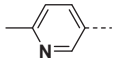	6.1	83, 94	39 ± 23	36	2.6	44	4.0
32	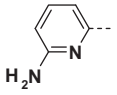	6.5	76, 95	63	91	1.5	50	3.3
33	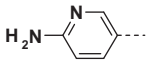	6.7	177	161				2.9
34	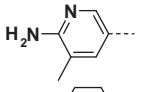	7.0	628					3.1
35	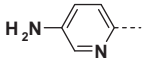	6.3	18, 45	168			238	3.9
36	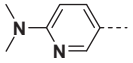	7.2	867	360				4.1
37	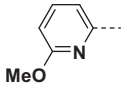	3.6	80, 124	50	39	24	78	6.1
38	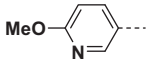	3.5	318	90	53		6	5.7
39	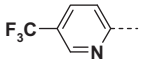	3.0	157	110	33		0.8	6.3
40		2.0	41, 46	136	11	3.3	434	4.7
41		1.2	20, 25	58	28	7.0	129	4.6
42	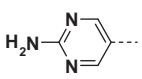	4.0	150	300				4.2

[a] $n \geqslant 2$: arithmetic mean ± standard deviation is reported.
[b] $T_{1/2}$ measured in human liver microsomes at 10 μM initial concentration.

Table 4
RLM metabolic stability and rat oral PK parameters for **24** and **32** at 10 mg/kg oral dose

Compds	RLM $T_{1/2}$ (min)[a]	C_{max} (μM)	AUC (μM·h)	Oral MRT (h)
24	9	1.23	0.87	0.5
32	21	0.99	1.18	3.4

[a] $T_{1/2}$ measured in rat liver microsomes (RLM) at 10 μM initial concentration.

Acknowledgments

We are grateful to Dr. Gordon Bolger, Christine Zouki and Josie De Marte for in vitro ADME data and to Colette Boucher, Michael Little and Serge Valois for analytical support. We thank Francine Liard, Manon Rhéaume and Hélène Montpetit for providing rat in vivo data. Nathalie Dansereau, Lisette Lagacé, Martin Marquis, Ginette McKercher and Louise Thauvette are acknowledged for profiling in HCV biological assays.

References and notes

1. (a) Choo, Q.-L.; Kuo, G.; Weiner, A. J.; Overby, L. R.; Bradley, D. W.; Houghton, M. *Science* **1989**, *244*, 359; (b) Lavanchy, D. *Liver Int.* **2009**, *29*, 74.
2. For reviews on NS5B inhibitors see (a) Beaulieu, P. L. *Expert Opin. Ther. Pat.* **2009**, *19*, 145; (b) Li, H.; Shi, S. T. *Future Med. Chem.* **2010**, *2*, 121; (c) Watkins, W. J.; Ray, A. S.; Chong, L. S. *Curr. Opin. Drug Discov. Devel.* **2010**, *13*, 441; For a review on inhibition of other HCV targets, see (a) Manns, M. P.; Foster, G. R.; Rockstroh, J. K.; Zeuzem, S.; Zoulim, F.; Houghton, M. *Nat. Rev. Drug Disc.* **2007**, *6*, 991; (b) Lange, C. M.; Sarrazin, C.; Zeuzem, S. *Aliment. Pharmacol. Ther.* **2010**, *32*, 14.
3. Farnik, H.; Mihm, U.; Zeuzem, S. *Liver Int.* **2009**, *29*, 23.
4. (a) Beaulieu, P. L. *Curr. Opin. Drug Discov. Devel.* **2006**, *9*, 618; (b) Rigat, K.; Wang, Y.; Hudyma, T. W.; Ding, M.; Zheng, X.; Gentles, R. G.; Beno, B. R.; Gao, M.; Roberts, S. B. *Antiviral Res.* **2010**, *88*, 197.
5. (a) Goulet, S.; Poupart, M.-A.; Gillard, J.; Poirier, M.; Kukolj, G.; Beaulieu, P. L. *Bioorg. Med. Chem. Lett.* **2010**, *20*, 196; (b) Beaulieu, P. L.; Dansereau, N.; Duan, J.; Garneau, M.; Gillard, J.; McKercher, G.; LaPlante, S.; Lagacé, L.; Thauvette, L.; Kukolj, G. *Bioorg. Med. Chem. Lett.* **2010**, *20*, 1825.
6. LaPlante, S. R.; Gillard, J. R.; Jakalian, A.; Aubry, N.; Coulombe, R.; Brochu, C.; Tsantrizos, Y. S.; Poirier, M.; Kukolj, G.; Beaulieu, P. L. *J. Am. Chem. Soc.* **2010**, *132*, 15204.
7. IC_{50} values were determined as previously described: (a) McKercher, G.; Beaulieu, P. L.; Lamarre, D.; LaPlante, S.; Lefebvre, S.; Pellerin, C.; Thauvette, L.; Kukolj, G. *Nucleic Acids Res.* **2004**, *32*, 422; EC_{50} determinations were performed using Huh-7 cells with a stable subgenomic HCV 1b replicon. The HCV RNA levels were normalized to total cellular RNA in this 72 h assay. The quantification of total RNA recovery allowed for an assessment of cellular homeostasis to eliminate the possibility of antiviral activity due to subtle toxic effects. For an overview and basic protocols on the use of HCV replicons, see (b) Lohmann, V. Hepatitis C: Methods and Protocols, 2nd edition In *Methods in Mol. Biol.*; Tang, H., Ed.; Humana Press, 2009; Vol. 510, p 145.
8. (a) Beaulieu, P. L.; Gillard, J.; Bykowski, D.; Brochu, C.; Dansereau, N.; Duceppe, J.-S.; Haché, B.; Jakalian, A.; Lagacé, L.; LaPlante, S.; McKercher, G.; Moreau, E.; Perreault, S.; Stammers, T.; Thauvette, L.; Warrington, J.; Kukolj, G. *Bioorg. Med. Chem. Lett.* **2006**, *16*, 4987; (b) Harper, S.; Pacini, B.; Avolio, S.; Di Filippo, M.; Migliaccio, G.; Laufer, R.; De Francesco, R.; Rowley, M.; Narjes, F. *J. Med. Chem.* **2005**, *48*, 1314; (c) Ontoria, J. M.; Martin Hernando, J. I.; Malancona, S.; Attenni, B.; Stansfield, I.; Conte, I.; Ercolani, C.; Habermann, J.; Ponzi, S.; Di Filippo, M.; Koch, U.; Rowley, M.; Narjes, F. *Bioorg. Med. Chem. Lett.* **2006**, *16*, 4026.
9. JChem 5.0.0 (http://www.chemaxon.com) was used for Log *P* predictions. The prediction method is based on the algorithm described in Viswanadhan, V. N.; Ghose, A. K.; Revankar, G. R.; Robins, R. K. *J. Chem. Inf. Comput. Sci.* **1989**, *29*, 163.
10. Lipinski, C. A.; Lombardo, F.; Dominy, B. W.; Feeney, P. J. *Adv. Drug Delivery Rev.* **1997**, *23*, 3.
11. Performed on amorphous TFA salts using the 24 h shaking flask method (pH 7.2 phosphate buffer).
12. Kalgutkar, A. S.; Gardner, I.; Obach, R. S.; Shaffer, C. L.; Callegari, E.; Henne, K. R.; Mutlib, A. E.; Dalvie, D. K.; Lee, J. S.; Nakai, Y.; O'Donnell, J. P.; Boer, J.; Harriman, S. P. *Curr. Drug Metab.* **2005**, *6*, 651.
13. Part 2: Beaulieu, P. L. *et al.* (accompanying paper).
14. Rorrer, L. C.; Hopkins, S. D.; Connors, M. K.; Lee, D. W., III; Smith, M. V.; Rhodes, H. J.; Uffelman, E. S. *Org. Lett.* **1999**, *1*, 1157.
15. All inhibitors in this study were purified to >95% homogeneity by reversed-phase HPLC and isolated as TFA salts. All compounds were characterized by mass spectrometry and gave ^{1}H NMR spectra consistent with expected structures.
16. Beaulieu, P. L.; Bös, M.; Bousquet, Y.; Fazal, G.; Gauthier, J.; Gillard, J.; Goulet, S.; LaPlante, S.; Poupart, M.-A.; Lefebvre, S.; McKercher, G.; Pellerin, C.; Austel, V.; Kukolj, G. *Bioorg. Med. Chem. Lett.* **2004**, *14*, 119.
17. LaPlante, S. R.; Jakalian, A.; Aubry, N.; Bousquet, Y.; Ferland, J.-M.; Gillard, J.; Lefebvre, S.; Poirier, M.; Tsantrizos, Y. S.; Kukolj, G.; Beaulieu, P. L. *Angew Chem., Int. Ed.* **2004**, *43*, 4306.
18. ACD/pK_a DB Version 11; Advanced Chemistry Development, Inc: Toronto, Canada, 2007.
19. Male Sprague–Dawley rats were fasted overnight and dosed by oral gavage at 10 mg/kg using 0.5% methocel and 0.3% Tween-80 as vehicle. Plasma samples from three animals were pooled at each time points (0–8 h) for analysis. Compound detection in plasma samples was performed following liquid–liquid extraction and HPLC analysis using UV detection.